

**Title**

Random sampling of the Green's Functions for reversible reactions with an intermediate state

**Authors' names**

Ianik Plante<sup>\*†§</sup>, Luc Devroye<sup>‡</sup>, Francis A. Cucinotta<sup>†</sup>

**Authors' affiliations**

\*Division of Space Life Sciences  
Universities Space Research Association  
3600 Bay Area Boulevard, Houston, TX 77058

†NASA Johnson Space Center  
Bldg 37, Mail Code SK  
2101 NASA Parkway, Houston, TX 77058

‡School of Computer Science  
McGill University  
3480 University Street, Montreal H3A 0E9 (Canada)

Email: [ianik.plante-1@nasa.gov](mailto:ianik.plante-1@nasa.gov)  
[Francis.A.Cucinotta@nasa.gov](mailto:Francis.A.Cucinotta@nasa.gov)  
[lucdevroye@gmail.com](mailto:lucdevroye@gmail.com)

§Corresponding Author:

Ianik Plante  
NASA Johnson Space Center  
2101 NASA Parkway  
Mail Code SK  
Houston TX 77058  
Office: 281 483-0968  
Fax: 281 483-3058

TITLE RUNNING HEAD

Random sampling of the Green's functions

**Receipt date**

January 28, 2013

## **Abstract**

Exact random variate generators were developed to sample Green's functions used in Brownian Dynamics (BD) algorithms for the simulations of chemical systems. These algorithms, which use less than a kilobyte of memory, provide a useful alternative to the table look-up method that has been used in similar work. The cases that are studied with this approach are 1) diffusion-influenced reactions; 2) reversible diffusion-influenced reactions and 3) reactions with an intermediate state such as enzymatic catalysis. The results are validated by comparison with those obtained by the Independent Reaction Times (IRT) method. This work is part of our effort in developing models to understand the role of radiation chemistry in the radiation effects on human body and may eventually be included in event-based models of space radiation risk.

## **Physics and Astronomy Classification Scheme (PACS) indexing codes**

87.15.A-	Theory, modeling, and computer simulation
87.15.ak	Monte Carlo simulations
82.37.Np	Single molecule reaction kinetics, dissociation, etc.
87.53.Ay	Biophysical mechanisms of interaction

## **1. Introduction**

Simulations based on the Green's functions of the diffusion equation (DE) have been used for years to study chemical reactions in solutions [1-10]. More recently, this approach has been used in radiation chemistry codes to simulate the radiolysis of water and aqueous solutions [11-12], chemical dosimeters [13] and to study of interaction of ligand molecules with receptors [14]. The purpose of this work is to propose and validate a sampling algorithm of the Green's function of the diffusion equation (DE), which is used to simulate chemistry in non-homogeneous systems. The algorithm is exact for 2-particles systems and requires less than 0.15 kilobytes of memory. The cases that are studied with this approach are 1) diffusion-influenced reactions; 2) reversible diffusion-influenced reactions and 3) reactions with an intermediate state such as enzymatic catalysis. The results are compared with those obtained with the independent reaction times (IRT) method. The performance of the algorithm was compared to table look-up methods which are the standard method used for this kind of simulations. This algorithm will be used in Brownian Dynamics codes to simulate the radiation chemistry of the radiolytic species (such as the free radical  $\cdot\text{OH}$ ) created by the interaction of ionizing radiation with water and eventually study DNA damage by the indirect effect.

## 2. Use of the diffusion equation in chemistry

### 2.1 Modeling of chemical reactions

The approach presented in this paper has been used to study complex problems such as reversible reactions with an intermediate state, which may be represented as follows [7]:



where  $k_a$  is the association rate constant,  $k_d$  is the complex dissociation rate constant and  $k_e$  is the products formation rate constant. The units of  $k_a$  are  $[\text{length}]^3[\text{time}]^{-1}$ , and the units of  $k_d$  and  $k_e$  are  $[\text{time}]^{-1}$ . As it is well known [8-9; 15], the probability distribution of the separation vector between two particles is a Green's function of the DE. Therefore, the DE for a three-dimensional system with

spherical symmetry is widely used to study chemical reactions of particles in solution [10]. This equation is [16]:

$$\frac{\partial p(r,t|r_0)}{\partial t} = \frac{D}{r^2} \frac{\partial}{\partial r} \left[ r^2 \frac{\partial}{\partial r} p(r,t|r_0) \right], r > R, \quad (2)$$

where  $R$  is the reaction radius,  $D$  is the sum of the diffusion coefficients of the particles, and  $r_0$  and  $r$  are the inter-particles distances at times 0 and  $t$ . The initial condition is [9]:

$$4\pi r_0^2 p(r,t|r_0) = \delta(r - r_0), r_0 > R, \quad (3)$$

where  $\delta$  is the Dirac's delta function. The boundary condition of this system at  $r=R$  is [7,9]:

$$4\pi R^2 D \left. \frac{\partial p(r,t|r_0)}{\partial r} \right|_{r=R} = k_a p(R,t|r_0) - k_d p(*,t|r_0). \quad (4)$$

where  $p(*,t|r_0)$  is the probability of the pair to be found in the reversibly bound state (\*). The time evolution of the pair in the reversibly bound state is given by

$$\frac{dp(*,t|r_0)}{dt} = k_a p(R,t|r_0) - (k_d + k_e) p(*,t|r_0). \quad (5)$$

The time evolution of the product state (\*\*) is given by

$$\frac{dp(**,t|r_0)}{dt} = k_e p(*,t|r_0). \quad (6)$$

## 2.2 Green's functions

The solution of the DE for the system described in the previous section (Green's function) is  $p(r,t|r_0)$ .

It is useful at this point to introduce the functions  $Erfc(x)$ ,  $W(x,y)$  and  $\Omega(x)$ <sup>1</sup>:

$$Erfc(x) \equiv \frac{2}{\sqrt{\pi}} \int_x^\infty e^{-\xi^2} d\xi, \quad (7a)$$

$$W(x,y) \equiv \exp(2xy + y^2) Erfc(x+y), \quad (7b)$$

$$\Omega(x) \equiv \exp(x^2) Erfc(x). \quad (7c)$$

---

<sup>1</sup> These functions may involve the product of a very large and a very small number, which may lead to overflow errors and loss of precision. The arguments of these functions can also be complex numbers. For complex arguments, the Faddeeva function is used [17].

The expression of  $p(r,t|r_0)$  and related functions are quite long. To simplify them, the variables

$\rho_r = (r - R)/\sqrt{4Dt}$ ,  $\rho_0 = (r_0 - R)/\sqrt{4Dt}$ ,  $\alpha' = \alpha\sqrt{Dt}$ ,  $\beta' = \beta\sqrt{Dt}$  and  $\gamma' = \gamma\sqrt{Dt}$  are introduced.

The Green's function (also called ‘‘Brownian propagator’’) is given by [7]:

$$4\pi r_0 p(r, t | r_0) = \frac{1}{\sqrt{4\pi Dt}} \left\{ \exp[-(\rho_r - \rho_0)^2] + \exp[-(\rho_r + \rho_0)^2] \right\} + \frac{\alpha(\beta + \alpha)(\gamma + \alpha)}{(\beta - \alpha)(\gamma - \alpha)} W(\rho_r + \rho_0, -\alpha') \quad (8)$$

$$+ \frac{\beta(\gamma + \beta)(\alpha + \beta)}{(\gamma - \beta)(\alpha - \beta)} W(\rho_r + \rho_0, -\beta') + \frac{\gamma(\alpha + \gamma)(\beta + \gamma)}{(\alpha - \gamma)(\beta - \gamma)} W(\rho_r + \rho_0, -\gamma')$$

where  $\alpha$ ,  $\beta$  and  $\gamma$  are the roots of a 3<sup>rd</sup> order polynomial. The coefficients of the polynomial are linked to the reaction rate constants as follows:

$$\alpha + \beta + \gamma = -(1 + k_a / k_D) / R, \quad (9a)$$

$$\alpha\beta + \beta\gamma + \gamma\alpha = (k_e + k_d) / D, \quad (9b)$$

$$\alpha\beta\gamma = -[(1 + k_a / k_D)k_e + k_d] / DR, \quad (9c)$$

and  $k_D = 4\pi RD$ . Since  $R > 0$  and the rate constant are all real and  $\geq 0$ , at least one of the root (which will be  $\alpha$  through this text) is real and negative. The roots  $\beta$  and  $\gamma$  are either real or complex conjugates.

The survival probability of a pair of particles  $Q(t|r_0)$  is calculated by integrating  $p(r,t|r_0)$  over the space outside the reaction radius  $R$ . This calculation yields:

$$Q(t | r_0) = \int_R^\infty 4\pi r^2 p(r, t | r_0) dr = 1 + \frac{(R\alpha + 1)(\beta + \alpha)(\gamma + \alpha)}{r_0 \alpha (\beta - \alpha)(\gamma - \alpha)} W(\rho_0, -\alpha') + \frac{(R\beta + 1)(\gamma + \beta)(\alpha + \beta)}{r_0 \beta (\gamma - \beta)(\alpha - \beta)} W(\rho_0, -\beta')$$

$$+ \frac{(R\gamma + 1)(\alpha + \gamma)(\beta + \gamma)}{r_0 \gamma (\alpha - \gamma)(\beta - \gamma)} W(\rho_0, -\gamma') - \left( \frac{1}{r_0} \right) \left( \frac{\alpha\beta + \beta\gamma + \gamma\alpha}{\alpha\beta\gamma} + R \right) \text{Erfc}(\rho_0) \quad (10)$$

For the simulations, the Green's function for the dissociation of a reversibly bound particle  $p(r,t|*)$  and the probabilities of transitions from one state to another  $p(*,t|r_0)$ ,  $p(**,t|r_0)$ ,  $Q(t|*)$ ,  $p(*,t|*)$  and  $p(**,t|*)$  are also needed. They are given in Appendix I.

These functions comprise several divisions by the roots and/or differences of the roots, which may lead to computational issues. The cases to consider are 1)  $\alpha \neq \beta \neq 0$ ,  $\gamma = 0$ ; 2)  $\alpha \neq 0$ ,  $\beta = \gamma \neq 0$ ; 3)  $\alpha \neq 0$ ,  $\beta = \gamma = 0$  and 4)  $\alpha = \beta = \gamma$ . The functions take different forms, which are presented in the supplemental material.

However, they are rarely an issue since  $R > 0$  implies that at least one of the roots is negative and

different from 0. For diffusion-controlled reaction ( $k_a > 0$ ,  $k_d = k_e = 0$ ),  $\beta = \gamma = 0$ . The Green's function is much simpler in this case [6, 18]:

$$4\pi r_0 p(r, t | r_0) = \frac{1}{\sqrt{4\pi Dt}} \left\{ \exp\left[-\frac{(r-r_0)^2}{4Dt}\right] + \exp\left[-\frac{(r+r_0-2R)^2}{4Dt}\right] \right\} + \alpha W\left(\frac{r+r_0-2R}{\sqrt{4Dt}}, -\alpha\sqrt{Dt}\right), \quad r \geq R, \quad (11)$$

where  $\alpha = -(k_a + 4\pi RD)/(4\pi R^2 D)$ . The survival probability of a pair of particles,  $Q(t|r_0)$ , is calculated by integrating  $p(r, t|r_0)$  over space outside the reaction radius  $R$ :

$$Q(t | r_0) = \int_R^\infty 4\pi r^2 p(r, t | r_0) dr = 1 + \frac{R\alpha + 1}{r_0 \alpha} \left[ W\left(\frac{r_0 - R}{\sqrt{4Dt}}, -\alpha\sqrt{Dt}\right) - \text{Erfc}\left(\frac{r_0 - R}{\sqrt{4Dt}}\right) \right]. \quad (12)$$

### 2.3. Discretization of time

A simulation is usually done in several time steps. During the simulation, after each time step, the state of the pair of particle or the inter-particle distance changes. However, the number of pairs in the different states as well as the distribution of distances of the pair at the end of the simulation should only depend on the sum of the time steps. In Appendix II, we show that the Green's functions are in accordance with this. This property of the Green's function is quite useful for the following reason. The values of  $r$  are distributed as  $p(r, \Delta t_1 | r_0)$  after the first time step. These values of  $r$  become the values of  $r_0$  for the next sampling. But we know that the values of  $r$  sampled after the next time step ( $\Delta t_2$ ) will be distributed as  $p(r, \Delta t_1 + \Delta t_2 | r_0)$ . Therefore, since the sampling algorithm in the second time step is used with different  $r_0$ , the algorithm is verified simultaneously for a whole range of the parameter  $r_0$ . The property further allows the verification of the algorithm for dissociation, since the distribution of  $r$  after two time steps comprises the contribution of the dissociated pairs of particles.

### 2.4 Simulations with the independent reaction times (IRT) method

A major problem encountered in radiation chemistry simulations is the calculation time. The main reason for this is that the number of possible interactions in a system comprising  $N$  particles is  $N(N-1)/2$ . This large number of interactions often makes the problem intractable, even for systems comprising a

relatively small number of particles. To overcome this problem, a method named independent reaction times (IRT) has been developed about 30 years ago [20-22], and has been widely used to calculate the radiolytic yields in aqueous solutions [23-26] and in chemical dosimeters [27-28]. This method is useful because it allows the calculation of radiolytic yields much faster than full step-by-step Brownian Dynamics simulations. However, the positions of the particles at each time step are not calculated; therefore, the extension of the IRT method to problems of interest to radiobiology such as DNA damage simulations may be difficult. In this work, the IRT method is used for comparison with the algorithm presented in this paper.

### 3. Methods

#### 3.1 Sampling of the Green's function with a reflective boundary

To construct a Brownian Dynamics algorithm it is necessary to generate random variates<sup>2</sup> (corresponding to inter-particle distance) from the Brownian propagator. Before discussing the case of diffusion-influenced reactions, an algorithm is proposed to generate random variates from the Green's function for the distance between two non-reacting particles, i.e.  $p(r, t | r_0)$  with  $k_a=0$ ,  $k_d=0$  and  $k_e=0$ . The boundary condition for this system is  $\partial p(r, t | r_0) / \partial r |_{r=R} = 0$  (the reflecting boundary condition); consequently, this particular Green's function will be noted  $p_{ref}(r, t | r_0)$ . As will be seen, the algorithm which will be obtained can be modified easily to Brownian propagators used to simulate chemical reactions. The distribution to sample is

$$4\pi r^2 p_{ref}(r, t | r_0) = \frac{r}{r_0 \sqrt{4\pi Dt}} \left\{ \exp\left[-\frac{(r-r_0)^2}{4Dt}\right] + \exp\left[-\frac{(r+r_0-2R)^2}{4Dt}\right] - \frac{\sqrt{4\pi Dt}}{R} W\left(\frac{r+r_0-2R}{\sqrt{4Dt}}, \frac{\sqrt{Dt}}{R}\right) \right\}, r \geq R. \quad (13)$$

This distribution is normalized, i.e.:

---

<sup>2</sup> The terminology given in the book of Devroye [29] regarding non-uniform random variate generation will be used here.

$$\int_{\mathbb{R}} 4\pi^2 p_{\text{ref}}(r, t | r_0) dr = 1. \quad (14)$$

The objective is to generate random variates  $X$  from  $f(x) \equiv 4\pi^2 p_{\text{ref}}(x, t | r_0)$ . This probability distribution is univariate, but includes four parameters  $r_0$ ,  $R$ ,  $D$  and  $t$ . As shown in the supporting document,  $f(r)$  can be written as a two parameters distribution. However, to avoid introducing more variables, the algorithm is given here in its original form.

Since  $W \geq 0$ , it is clear that  $f(x) \leq h(x)$ , where

$$h(x) = \frac{x}{r_0 \sqrt{4\pi Dt}} \left\{ \exp\left[-\frac{(x-r_0)^2}{4Dt}\right] + \exp\left[-\frac{(x+r_0-2R)^2}{4Dt}\right] \right\}, x \geq R. \quad (15)$$

Therefore, von Neumann's rejection method [29-31] can be used. The rejection method is a well-known general technique to generate random variates of the probability distribution  $p(x)$ , which does not require that the cumulative distribution function (the indefinite integral of  $p(x)$ ) be computable. To use this technique, we assume that  $p(x) \leq Cg(x)$ , where  $C$  is a proportionality constant such as  $C \geq 1$  and  $g(x)$  is a probability distribution for which random variates  $X$  distributed as  $g(x)$  can be easily generated. To generate random variates distributed as  $p(x)$ , a uniformly distributed random number  $U$  between 0 and 1 and a random variate  $X$  distributed as  $g(x)$  are generated. The value of  $X$  is accepted if the condition  $UCg(X) \leq p(X)$  is verified; otherwise, a new set of  $U$  and  $X$  are generated until the condition is true. From a geometric perspective, points are generated in the 2D plane bounded by the curve  $Cg(x)$  and the domain of  $g(x)$ ; the points are accepted are those which fall under  $p(x)$ .

In the actual problem, since  $f(x)$  is bounded from above by the first two terms ( $h$ ), the third (negative) term is ignored at this moment. The function  $h$  can be rewritten as the sum of four terms, which, after rearrangement and truncation to the positive ranges, are:

$$h_1(r) = \frac{r-r_0}{r_0 \sqrt{4\pi Dt}} \exp\left[-\frac{(r-r_0)^2}{4Dt}\right] \times 1_{[r \geq r_0]}, \quad (16a)$$

$$h_2(r) = \frac{r+r_0-2R}{r_0\sqrt{4\pi Dt}} \exp\left[-\frac{(r+r_0-2R)^2}{4Dt}\right] \times 1_{[r \geq R]}, \quad (16b)$$

$$h_3(r) = \frac{r_0}{r_0\sqrt{4\pi Dt}} \exp\left[-\frac{(r-r_0)^2}{4Dt}\right] \times 1_{[r \geq R]}, \quad (16c)$$

$$h_4(r) = \frac{2R-r_0}{r_0\sqrt{4\pi Dt}} \exp\left[-\frac{(r+r_0-2R)^2}{4Dt}\right] \times 1_{[r \geq R]} \times 1_{[r_0 \leq 2R]}, \quad (16d)$$

where  $\mathbf{1}_{[\text{condition}]}$  takes the value 1 when the condition is true, and 0 when it is false. Also define

$$h'_3(r) = \frac{r_0}{r_0\sqrt{4\pi Dt}} \exp\left[-\frac{(r-r_0)^2}{4Dt}\right] \times 1_{[r \leq R]}. \quad (17)$$

Thus,  $f(r) \leq h(r) \stackrel{\text{def}}{=} \sum_i h_i(r)$ . It is possible to generate a random variate with density proportional to  $h$  easily, since  $h$  is a mixture of known probability distribution functions. The weights of the contributions of  $h_1$ ,  $h_2$  and  $h_3+h_4$  are obtained by integration:

$$p_1 = \int h_1(y) dy = \sqrt{\frac{Dt}{\pi r_0^2}}, \quad (18a)$$

$$p_2 = \int h_2(y) dy = \sqrt{\frac{Dt}{\pi r_0^2}} \exp\left[-\frac{(R-r_0)^2}{4Dt}\right], \quad (18b)$$

$$p' = \int (h_3(y) + h_4(y)) dy = \Phi\left(\frac{r_0-R}{\sqrt{2Dt}}\right) + 1_{[r_0 \leq 2R]} \frac{2R-r_0}{r_0} \Phi\left(\frac{R-r_0}{\sqrt{2Dt}}\right), \quad (18c)$$

where  $\Phi(x)$  is the normal distribution function:

$$\Phi(x\sqrt{2}) = 1 - \text{Erfc}(x) / 2. \quad (19)$$

Generating a random variate  $X$  with density proportional to  $h$  is straightforward, since  $h_1$  and  $h_2$  are the Rayleigh and tail of Rayleigh distributions [29]. Therefore, the following algorithm (given in the form of a pseudo-code) can be used:

**Algorithm 1a**

Compute  $p_1, p_2$  and  $p'$ . Set  $s = p_1 + p_2 + p'$ .

Generate a uniform  $[0,1]$  random variate  $U$

If  $sU \in [0, p_1]$ , then set  $X \leftarrow r_0 + \sqrt{4DtE}$ , where  $E$  is standard exponential<sup>3</sup>.

If  $sU \in (p_1, p_1 + p_2]$ , then set  $X \leftarrow 2R - r_0 + \sqrt{(r_0 - R)^2 + 4DtE}$ , where  $E$  is standard exponential.

If  $sU \in (p_1 + p_2, s]$ , then let  $X$  be a random variate with density proportional to  $h_3 + h_4$ .

Return  $X$ .

To generate a random variate with density proportional to  $h_3 + h_4$ , it is noted that  $h_4(r) \leq h_3'(2R - r)$  for  $r \geq R$ . But  $h_3 + h_3'$  is identical to the standard normal density with variance  $2Dt$  centered at  $r_0$ . Therefore, an algorithm based on the rejection method can be used to generate a random variate from  $h_3 + h_4$ :

**Algorithm 1b:**

```
Repeat {
  Generate  $N$  standard normal4,  $U$  uniform on  $[0,1]$ 
  Set  $X \leftarrow r_0 + \sqrt{2Dt}N$ .
} Until  $X > R$ , or jointly  $X < R$ ,  $r_0 < 2R$  and  $U \leq (2R - r_0)/r_0$ .
In the former case, return  $X$ .
In the latter case, return  $2R - X$ .
```

where Repeat {...} Until is a conditional "Do" loop. Finally, the overall algorithm generates pairs  $(X, U)$  with  $X$  having density proportional to  $h$  and  $U$  uniform  $[0,1]$  until  $Uh(Y) \leq f(Y)$ , and returns  $Y$ . The expected number of iterations is  $p_1 + p_2 + p'$ . As it was implicitly shown,  $p' \leq 1$  (Eq. 18c), so the contribution from  $h_3 + h_4$  is minor.

### 3.2 Sampling of the Green's function for diffusion-influenced reactions

The Green's function for diffusion-influenced reactions is similar to  $p_{ref}(r, t | r_0)$ . Because  $k_a > 0$ ,  $\alpha < 0$  and the Green's function is bounded from above by  $p_{ref}(r, t | r_0)$ . Therefore, **algorithm 1** can be used, replacing  $f(X)$  in final rejection step by the Green's function for diffusion-influenced reactions.

### 3.3 Sampling of the Green's function for the general case

---

<sup>3</sup> A standard exponential random variate is distributed as  $p(x) = \exp(-x)$ ,  $x \geq 0$ . It can be generated from a uniform random number  $U$  between 0 and 1 by using  $E = -\log(U)$ .

The Green's function for more complex systems such as those used for reactions with an intermediate state, considering the range of the parameters used, is also bounded from above by  $p_{ref}(r, t|r_0)$ . Therefore, **algorithm 1** can also be used by replacing  $f(X)$  in the final rejection step. However, in addition to sampling the propagator  $p(r, t|r_0)$ , the BD algorithm require sampling the Green's function for the dissociation of a bounded pair  $p(r, t|*)$ . This can be done by writing  $p(r, t|*)$  in a form suitable for rejection sampling, i.e. with a Gaussian function in evidence:

$$p(r, t|*) = \frac{k_d}{4\pi r R D} \exp\left[-\frac{(r-R)^2}{4Dt}\right] \left[ \frac{\alpha}{(\beta-\alpha)(\gamma-\alpha)} \Omega\left(\frac{r-R}{\sqrt{4Dt}} - \alpha\sqrt{Dt}\right) + \frac{\beta}{(\gamma-\beta)(\alpha-\beta)} \Omega\left(\frac{r-R}{\sqrt{4Dt}} - \beta\sqrt{Dt}\right) + \frac{\gamma}{(\alpha-\gamma)(\beta-\gamma)} \Omega\left(\frac{r-R}{\sqrt{4Dt}} - \gamma\sqrt{Dt}\right) \right], \quad (20)$$

where  $r \geq R$ . The distribution function to sample is  $4\pi r^2 p(r, t|*)$ , which can be written as the product of the functions  $g(r)$  and  $h(r)$ :

$$g(r) = r \exp\left[-\frac{(r-R)^2}{4Dt}\right], \quad (21)$$

$$h(r) = \frac{\alpha}{(\beta-\alpha)(\gamma-\alpha)} \Omega\left(\frac{r-R}{\sqrt{4Dt}} - \alpha\sqrt{Dt}\right) + \frac{\beta}{(\gamma-\beta)(\alpha-\beta)} \Omega\left(\frac{r-R}{\sqrt{4Dt}} - \beta\sqrt{Dt}\right) + \frac{\gamma}{(\alpha-\gamma)(\beta-\gamma)} \Omega\left(\frac{r-R}{\sqrt{4Dt}} - \gamma\sqrt{Dt}\right). \quad (22)$$

The function  $g(r)$  is a mixture of know probability distributions, for which a sampling algorithm can be developed easily. The function  $h(r)$  comprises three terms with  $\Omega(x)$ . But since the value of  $\Omega(x)$  ranges from 0 to 1 for  $x \geq 0$ ,  $h(r)$  can be used as the rejection function. The function  $g(r)$  can be written as the sum of two functions:

$$g_1(r) = (r-R) \exp\left[-\frac{(r-R)^2}{4Dt}\right] \times 1_{[r>R]}, \quad (23)$$

$$g_2(r) = (R) \exp\left[-\frac{(r-R)^2}{4Dt}\right] \times 1_{[r>R]}. \quad (24)$$

The function  $g(r) = g_1(r) + g_2(r)$  is not normalized. However, it is not an issue for sampling since only the relative contributions of  $g_1$  and  $g_2$  are needed. They are calculated by integration:

---

<sup>4</sup> A standard normal random variate is distributed as  $p(x) = (2\pi)^{-1/2} \exp(-x^2/2)$ . A normal random variate  $N$  can be generated from two random numbers uniformly distributed between 0 and 1 ( $U_1$  and  $U_2$ ) by using the Box-Muller method, i.e.  $N = \sqrt{-2\ln U_1} \cos(2\pi U_2)$  [31].

$$p_1 = \int_R^{\infty} g_1(r) dr = 2Dt, \quad (25)$$

$$p_2 = \int_R^{\infty} g_2(r) dr = \sqrt{\pi R^2 Dt}. \quad (26)$$

Therefore variates  $X$  distributed as  $g(X)$  can be generated by using the following algorithm:

**Algorithm 2**

Compute  $p_1$  and  $p_2$

Generate  $U$  uniform on  $[0,1]$

If  $U < p_1/(p_1+p_2)$  Set  $X \leftarrow R + \sqrt{-4Dt \log(V)}$ , where  $V$  is uniform on  $[0,1]$

Else set  $X \leftarrow R + |N| \sqrt{2Dt}$ , where  $N$  is standard normal.

Return  $X$

The sampled values ( $X$ ) are then used in the rejection function  $h(X)$ , for which the maximum value  $h_{max}$  is needed. But since  $h(r)$  is the sum of three terms comprising  $\Omega(x)$ , for which the value ranges from 0 to 1, the maximum value of  $h(r)$  is given by sum and/or differences of the coefficients. However, the sum of the coefficients is 0; thus, the sum of the absolute value of the coefficients, i.e.  $h_{max} = |\alpha/(\beta-\alpha)(\gamma-\alpha)| + |\beta/(\gamma-\beta)(\alpha-\beta)| + |\gamma/(\alpha-\gamma)(\beta-\gamma)|$  is used. Therefore, **algorithm 2** can be used with a rejection method using  $h(r)$  and  $h_{max}$ , i.e. the sampled values  $X$  are accepted if  $Vh_{max} \leq h(X)$ , where  $V$  is a random number uniformly distributed between 0 and 1.

### 3.4 Look-up table methods

To evaluate the performance of the algorithm, look-up tables were built and used to generate values of  $R$ . The Green's function  $p(r,t|r_0)$  is univariate, but with two parameters. By fixing the time step, the number of parameters is reduced to one but the tables are different for different values of  $r_0$ . Therefore one dimensional tables were built as in ref. [7], depending on which simulation is done. The table should be recalculated for each different value of  $r_0$ . The dissociation Green's function  $p(r,t|*)$  is univariate for a fixed time step; therefore, a one-dimensional table can be built using Equation C3b of ref. [7].

### 3.5 The IRT method

The IRT method is widely used in radiation chemistry [23-28]. A detailed description of this method is beyond the scope of this paper; therefore, only the most important points will be given here. Briefly, knowing the initial positions of the particles in the system, a reaction time is sampled for each pair of particles by solving numerically the equation

$$\frac{R\alpha + 1}{r_0\alpha} \left[ W\left(\frac{r_0 - R}{\sqrt{4Dt}}, \alpha\sqrt{Dt}\right) - \text{Erfc}\left(\frac{r_0 - R}{\sqrt{4Dt}}\right) \right] = U, \quad (27)$$

where  $U$  is a random number uniformly distributed between 0 and 1. This time is infinite (and therefore not considered) if a reaction is not possible. Similarly, a reaction time is obtained for first-order processes by sampling an exponential distribution with parameter given by the inverse of the dissociation rate constant. The reaction times are sorted and the reactions are processed according to the time in the list, by deleting reactants and adding reaction products. The reaction time list is updated after each reaction. The reactions are done until the final time is reached. With this method, the competition between reactions is described via sorting the reaction times, and no provision is made to account for spatial correlations that could exist between reactants [24].

#### 4. Results and discussion

The simulation results are presented in this section.

##### 4.1 Reflective boundary

Since  $k_a = k_d = k_e = 0$ ,  $\alpha = -1/R$  and  $\beta = \gamma = 0$ . As expected,  $Q(t|r_0) = 1$  since there are no reactions of particles. In Figure 1, the function  $4\pi r^2 p_{ref}(r, t|r_0)$  with parameters  $R = 1$  and  $r_0 = 1.5$  is plotted. The region  $r < R$  is forbidden.

*Figure 1*

The Brownian propagator has been sampled 1,000,000 times using **algorithm 1**, and the sampled  $r$  values were stored in histograms. The number of counts in each histogram “bin” are normalized and

plotted as points for comparison with the analytical Green's functions. The number of histories is chosen to ensure results convergence in a reasonable calculation time. A  $\chi^2$  test was performed using 10,000, 100,000 and 1,000,000 histories to evaluate if the sampled distribution is different from the analytical predictions. In all cases, the  $\chi^2$  statistics is  $<110$  for 88 degrees of freedom, indicating that the distributions are not statistically different if the 95% threshold value is used. However, to avoid a large dispersion of the sampled values, 1,000,000 histories are used for all the simulations done in this paper.

The first calculation is done for  $t=1$  with the initial value of  $r_0=1.5$ . The calculation for  $t=2$  is done by sampling the Green's function using the  $r$  values generated by the previous calculations as initial  $r_0$ . Therefore the points at  $t=2$  are the result of two consecutive sampling of the Green's function. Similar results may be obtained by sampling the Green's function once with  $t=2$ . The results for  $t=4, 8, 16$  and  $32$  can be obtained in the same way, either by sampling the Green's function directly or by using multiple consecutive sampling with any combination of  $\Delta t$  which gives a total time of  $t$ .

#### 4.2 Diffusion-influenced chemical reactions

In this case,  $k_a > 0$ ,  $k_d = k_e = 0$ . Since  $\alpha < -1/R$ ,  $Q(t|r_0) < 1$ , indicating reaction of particles over time. In Figure 2a, the function  $4\pi r^2 p(r, t|r_0)$  (Eq. 12) with  $R=1$ ,  $D=1$ ,  $k_a=4\pi RD$  ( $\alpha=-2$ ) and  $r_0=1.5$  is plotted. In Figure 2b, the average free particle count (given by  $2Q(t|r_0)$ ) are plotted for  $k_a=1x4\pi RD$  ( $\alpha=-2$ ),  $k_a=2x4\pi RD$  ( $\alpha=-3$ ),  $k_a=4x4\pi RD$  ( $\alpha=-5$ ) and  $k_a=100x4\pi RD$  ( $\alpha=-101$ ). Results obtained with the IRT method are also shown.

Figure 2

The Green's functions are very similar to those depicted in Figure 1. The maximum of all corresponding curves are lower, due to reaction of particles. As in the previous section, 1,000,000 histories of pair of particles are simulated. In this case, the survival of a pair of particles is assessed at each time step by looking if  $Q(t|r_0) < U$ , where  $U$  is a uniformly distributed random number between 0

and 1. If a pair reacts, it is considered in a bound state and the Brownian propagator is not sampled anymore. Otherwise, a new value of  $r$  is obtained by sampling the Brownian propagator using **algorithm 1**. The first calculation is done for  $t=1$  using the initial value of  $r_0=1.5$ . As in the previous section, the calculation for  $t=2$  is done by sampling the Green's function using the  $r$  values generated by the previous calculations as initial  $r_0$  on surviving pairs of particles. Therefore the points at  $t=2$  are the result of two consecutive sampling of the Green's function. Similar results (not shown) may be obtained by sampling the Green's function once with  $t=2$ . The results for  $t=4, 8, 16$  and  $32$  can also be obtained by using multiple sampling of the Green's function, as previously described.

In the long time limit,  $Q(t \rightarrow \infty | r_0)$  takes the form

$$\lim_{t \rightarrow \infty} Q(t | r_0) \sim 1 - \frac{R\alpha + 1}{r_0 \alpha} \left[ 1 + \frac{1}{\alpha \sqrt{\pi D t}} \right]. \quad (28)$$

As shown in Figure 2b, the average particle count plateaus at the predicted values for  $t \rightarrow \infty$ . In the limit of diffusion-controlled reactions ( $k_a \rightarrow \infty$ ),  $Q(t \rightarrow \infty | r_0) \rightarrow 1 - R/r_0$ .

### 4.3 Reversible reaction

In this section, the case where  $k_a > 0$ ,  $k_d > 0$  and  $k_e = 0$  is considered. Even if  $k_e = 0$ , it is possible for  $\beta$  and  $\gamma$  to be complex conjugates, so the general equations for the Green's functions should be used.

#### Figure 3

In Figure 3a, the Green's functions  $4\pi r^2 p(r, t | r_0)$  (Eq. 8) are shown at  $t=1, 2, 4, 8, 16$  and  $32$  for  $R=1$ ,  $D=1$ ,  $k_a=10(4\pi RD)$ ,  $k_d=36$ , and  $r_0=1.5$  ( $\alpha=-2$ ,  $\beta=-6$ ,  $\gamma=-3$ ). The Green's functions are very similar to those obtained in the previous section. The time discretization property is also verified, i.e. the results at  $t=2$  are the simulation of two consecutive sampling of the Green's functions. As in diffusion-controlled reactions, the program verifies if the free pairs are in a bound state after a time step by using  $Q(t | r_0)$ . At the second (and subsequent) time steps, a bound pair may dissociate with probability  $Q(t | *)$ . If the pair dissociates, a new distance between particles is found by sampling  $4\pi r^2 p(r, t | *)$  using **algorithm 2**.

Therefore, the simulation points depicted in Figure 3 for  $t \geq 2$  include contributions of the sampling of the Green's function for the pair in the bound state. In Figure 3b, the average free and reversibly bound particle count (given by  $2Q(t|r_0)$  and  $p(*,t|r_0)$ ) are plotted as a function of time for  $k_a=5(4\pi RD)$ ,  $R=1$ ,  $D=1$ ,  $r_0=1.5$  and three values of  $k_d$ . The results from the IRT simulations are also shown; they also match the results obtained with the Green's function with excellent agreement. It should be noted that the forward and backward (dissociation) reactions are treated separately by IRT, and that the Green's function given by Equation (8) is not used by IRT.

As noted by Agmon [3], since the particles diffuse away from each other, the pair will always dissociate in the long-time limit. The long-time behavior of the survival probability is given by [6]:

$$\lim_{t \rightarrow \infty} Q(t|r_0) \sim \frac{k_a}{k_d} \frac{1}{(4\pi Dt)^{3/2}}. \quad (29)$$

#### 4.4 Reversible reaction and enzyme catalysis

This is the general case with  $k_a > 0$ ,  $k_d > 0$  and  $k_e > 0$ , for which  $\beta$  and  $\gamma$  can be complex conjugates. The simulation of these reactions is similar to those of the previous section. In this case, the probabilities for the possible states of a pair of particles initially at distance  $r_0$  are given by  $Q(t|r_0)$  (free),  $p(*,t|r_0)$  (reversibly bound) and  $p(**,t|r_0)$  (reaction). For free pairs, the distance is sampled by using **algorithm 1**. Similarly, the state of a reversibly bound pair after a time step is determined by using  $Q(t|*)$  (free),  $p(*,t|*)$  (reversibly bound) and  $p(**,t|*)$  (reaction).

#### Figure 4

In Figure 4a, the Green's functions  $4\pi r^2 p(r,t|r_0)$  (Eq. 8) are shown at  $t=1, 2, 4, 8, 16$  and  $32$  for  $R=1$ ,  $D=1$ ,  $k_a=14(4\pi RD)$ ,  $k_d=65$ ,  $k_e=1$ , and  $r_0=1.5$  ( $\alpha=-8$ ,  $\beta=-2$  and  $\gamma=-5$ ). As in previous sections, the data shown for  $t=2$  and subsequent times are obtained as the result of several consecutive sampling of the Green's functions. Once again, the agreement between results of sampling and analytical Green's functions is excellent at all times values. In Figure 4b, the average count of free, reversibly bound and

irreversibly bound particles (given by  $2Q(t|r_0)$ ,  $p(*,t|r_0)$  and  $p(**,t|r_0)$ ) are plotted for  $R=1$ ,  $D=1$ ,  $k_a=4\pi RD$ ,  $k_d=1$ ,  $r_0=1.5$  and different values of  $k_e$ . Results calculated by using the IRT method are also shown. The agreement of the results from IRT with the analytical functions is also excellent. In the long time limit, as shown in Figure 4b,  $Q(t \rightarrow \infty | r_0) \sim (R/r_0)k_e(k_d/k_D)/(k_d+k_e(1+k_d/k_D))$ .

#### 4.5 Performance and limitations of the algorithms

Usually, table look-up methods are used to generate samples from the Green's functions of the DE in Brownian Dynamics simulations [7,32-33]. In Table 1, the simulation times of the algorithms presented in the paper are compared with the simulation obtained with table look-up method.

*Table 1*

In Table 2, the  $\chi^2$  values were obtained by comparing the simulation results with the analytical Green's function. This calculation is done to evaluate if the simulated distributions are significantly different from the expected distributions. The  $\chi^2$  critical value for 88 degrees of freedom is  $\sim 110.8$ , using a probability value of 0.05. Therefore, a  $\chi^2$  value below the critical value indicates that the distributions are not significantly different.

*Table 2*

The simulations were performed using an Intel Xeon CPU E5430 @ 2.66 GHz. The simulation times obtained with our algorithm are to the values obtained with algorithms for sampling the Green's functions in 1D [14]. The simulation time for both our algorithm and table methods increases with the complexity of the Green's functions. The rate constants for the simulations were chosen such as the roots  $\alpha$ ,  $\beta$  and  $\gamma$  are real. A simulation was also done with complex values of  $\beta$  and  $\gamma$  for comparison. The simulation time is significantly higher for this simulation, because the imaginary part of  $W$  needs to

be calculated<sup>5</sup>. The simulation time for the table look-up method also increases with the resolution of the table. We found that a resolution of 500 and 1000 bins are not sufficient to keep the  $\chi^2$  values below the threshold of 110.8, but it is possible to do so by using 2,000 bins. Increasing the resolution of the table to 4,000 bins doesn't yield better results, but the calculation time significantly increases.

We have tried to evaluate the memory needed by our method and by the look-up tables. The results are shown in Table 3.

*Table 3*

The memory usage of the algorithms was done by counting the number of bytes needed by each variables used, knowing that double precision number requires 8 bytes of memory. The tables for  $W$  comprise complex numbers in double precision. The table for the look-up method comprises real numbers in double precision. The memory requirement of the table methods are not that high, but it may increase quickly if the tables are pre-calculated to account for the different parameters. For example, in a system comprising several kind of particles interacting with different reaction rate constants, the tables should be calculated for each values of  $\alpha$ ,  $\beta$  and  $\gamma$ .

#### *4.6 Applicability of the Green's functions*

The Green's functions used here are exact only for systems comprising 2 particles. The problem becomes much more complex when there are more than 2 particles are involved, and the Green's functions are no longer exact. If more than two particles are close to each other, the numerical Green's function can be obtained numerically, and table look-up methods can be used [33]. If particles are too far from each other, the particles will not react and therefore it is not necessary to sample the propagator.

---

<sup>5</sup> Although the imaginary terms of the terms of the Green's functions cancels, they need to be calculated because the coefficients of  $W$  are complex.

The decision is usually based on the “reaction zone” of a particle, which is defined near each particle to determine if it is necessary to use the sampling algorithms [32]. The condition  $r_0 < [R + 8(2Dt)^{1/2}]$  is used in ref. [29] to define the reaction zone.

If there is an electrostatic interaction between the particles e.g. a Coulomb potential, it is necessary to use the solution of the Debye-Smoluchowski equation [34]. However, in systems that are of interest to radiobiology, such as the DNA damage by the radical species created during the radiolysis of water, the majority of reactions is partially diffusion-controlled and can be simulated with the approach given in this paper. The only notable exception is the reaction  $H^+ + e^-_{aq} \rightarrow H\cdot$  [11], for which a numerical calculation may be necessary considering the complexity of the analytical Green's function [34].

## 5. Conclusion

The approach based on Green's function is used in many codes to simulate chemical reactions in a system comprising particles. The sampling of the Brownian propagators are therefore of great interest for such codes. The Green's functions for some cases such as enzymatic catalysis are quite complex; however, it is possible to use the relatively simple algorithms presented in this paper to simulate the evolution in time and space of pair of particles. In general, the performance of our algorithm is similar or better than table methods. Table methods usually necessitate some memory to hold the pre-calculated data, which may become problematic when the table has more than one dimension [33].

In radiation chemistry, the IRT method was used to calculate the yields of the radiolytic species in solutions [22-26] and also in chemical dosimeters [27-28]. The IRT method is based on the survival probability of pair of particles, and the competition between reactions are taken into consideration by sorting the sampled reaction time. Although the purpose of this article is not the validation of the IRT method, it is interesting to note that our simulation results are in excellent agreement with those predicted by IRT. In fact, to our knowledge, the comparison of the predictions of the analytical Green's

functions with the IRT results for 2-particle systems with reversible diffusion-influenced reactions or enzyme catalysis has not been attempted before.

Because the algorithms are simple and use only a few kilobytes of memory, they can possibly be implemented on a general-purpose graphic processing unit (GPGPU). GPGPU is a computing device operating as a co-processor to the main central process unit (CPU). GPGPUs comprise up to several hundred cores and have their own memory. They are used to compute functions which are executed a large number of times, but independently on different data. Therefore, the algorithms could be implemented on a GPGPU to simulate a chemical system comprising different types of particles. This work should be useful for chemistry codes that are based on this approach to study DNA damage, which may eventually be included in event-based models of space radiation risk [35].

## Acknowledgements

This work was supported by the NASA Space Radiation Risk Assessment Project. We would also like to thank Drs. Noam Agmon and Dr. Soohyung Park for useful correspondence.

## References

- [1] A.L. Edelman, N. Agmon, Brownian dynamics simulations of reversible reactions in one dimension, *J. Chem. Phys.* 99 (1993) 5396-5404. doi: 10.1063/1.465983
- [2] A.L. Edelman, N. Agmon, Equilibration in reversible bimolecular reactions, *J. Phys. Chem.* 99 (1995) 5389-5401. doi: 10.1021/j100015a024
- [3] N. Agmon, Diffusion with back reaction. *J. Chem. Phys.* 81 (1984) 2811-2817. doi: 10.1063/1.447954
- [4] H. Kim, K.J. Shin, N. Agmon, Excited-state reversible geminate recombination with quenching in one dimension, *J. Chem. Phys.* 111 (1999) 3791-3799. doi: 10.1063/1.479682
- [5] N. Agmon, A.V. Popov, Unified theory of reversible target reactions, *J. Chem. Phys.* 119 (2003) 6680-6690. doi: 10.1063/1.1603717
- [6] H. Kim, K.J. Shin, Exact solution of the reversible diffusion-influenced reaction for an isolated pair in three dimensions, *Phys. Rev. Lett.* 82 (1999) 1578-1581. doi: 10.1103/PhysRevLett.82.1578
- [7] S. Park, N. Agmon, Theory and simulation of diffusion-controlled Michaelis–Menten kinetics for a static enzyme in solution, *J. Phys. Chem. B* 112 (2008) 5977-5987. doi: 10.1021/jp075941d

- [8] J.S. van Zon, P.R. ten Wolde, Green's function reaction dynamics: A particle-based approach for simulating biochemical networks in time and space, *J. Chem. Phys.* 123 (2005) 234910. doi: 10.1063/1.2137716
- [9] H. Kim, K.J. Shin, N. Agmon, Diffusion-influenced reversible geminate recombination in one dimension. II. Effect of a constant field. *J. Chem. Phys.* 114 (2001) 3905-3912. doi: 10.1063/1.1344607
- [10] A.V. Popov, N. Agmon, Exact solution for the geminate ABCD reaction, *J. Chem. Phys.* 117 (2002) 5770-5779. doi: 10.1063/1.1501127
- [11] I. Plante, A Monte-Carlo step-by-step simulation code of the non-homogeneous chemistry of the radiolysis of water and aqueous solutions. Part I: theoretical framework and implementation, *Radiat. Env. Biophys.* 50 (2011) 389-403. doi: 10.1007/s00411-011-0367-8
- [12] I. Plante, A Monte-Carlo step-by-step simulation code of the non-homogeneous chemistry of the radiolysis of water and aqueous solutions. Part II: Calculation of radiolytic yields under different conditions of LET, pH and temperature, *Radiat. Env. Biophys.* 50 (2011) 389-403. doi: 10.1007/s00411-011-0368-7
- [13] I. Plante, T. Tippayamontri, N. Autsavapromporn, J. Meesungnoen, J.-P. Jay-Gerin, Monte-Carlo simulation of the radiolysis of the ceric sulfate dosimeter by low-LET radiation, *Can. J. Chem.* 90 (2012) 717-723. doi: 10.1139/v2012-052
- [14] I. Plante, F.A. Cucinotta, Model of the initiation of signal transduction by ligands in a cell culture: Simulation of molecules near a plane membrane comprising receptors, *Phys. Rev. E.* 84 (2011), 051920. doi: 10.1103/PhysRevE.84.051920
- [15] S.A. Rice, *Comprehensive Chemical Kinetics*, Vol. 25 (Diffusion-limited Reactions), Elsevier, Amsterdam, 1985.
- [16] E.B. Krissinel, N. Agmon, Spherical symmetric diffusion problem, *J. Comput. Chem.* 17 (1995) 1085-1098. doi: 10.1002/(SICI)1096-987X(19960715)17:9<1085::AID-JCC1>3.0.CO;2-O
- [17] G.P. Poppe, C.M.J. Wijers, Algorithm 680: evaluation of the complex error function, *ACM Trans. Math Software* 16 (1990) 47. doi: 10.1145/77626.77630
- [18] H.S. Carslaw, J.C. Jaeger, *Conduction of Heat in Solids*, Oxford University Press, Oxford, 1959.
- [19] A. Papoulis, *Probability, Random Variables and Stochastic Processes*. McGraw Hill, 3<sup>rd</sup> edition, 1991.
- [20] N.J.B. Green, M.J. Pilling, S.M. Pimblott, P. Clifford, Stochastic modeling of fast kinetics in a radiation track, *J. Phys. Chem.* 94 (1990) 251-258. doi: 10.1021/j100364a041
- [21] P. Clifford, N.J.B. Green, M.J. Pilling, Stochastic model based on pair distribution functions for reaction in a radiation-induced spur containing one type of radical, *J. Phys. Chem.* 86 (1982) 1318-1321. doi: 10.1021/j100397a021
- [22] P. Clifford, N.J.B. Green, M. Oldfield, M.J. Pilling, S.M. Pimblott, Stochastic models of multi-species kinetics in radiation-induced spurs, *J. Chem. Soc., Faraday Trans.* 1 82 (1986) 2673-2689. doi:10.1039/f19868202673
- [23] S.M. Pimblott, J.A. LaVerne. Stochastic simulation of the electron radiolysis of water and aqueous solutions. *J. Phys. Chem. A* 101 (1997) 5828-5838. doi: 10.1021/jp970637d
- [24] T. Goulet, M.-J. Fraser, Y. Frongillo, J.-P. Jay-Gerin. On the validity of the Independent Reaction Times approximation for the description of the nonhomogeneous kinetics of liquid water radiolysis. *Radiat. Phys. Chem.* 51 (1998) 85-91. doi: 10.1016/S0969-806X(97)00060-1

- [25] Y. Frongillo, T. Goulet, M.-J. Fraser, V. Cobut, J.P. Patau, J.-P. Jay-Gerin, Monte Carlo simulation of fast electron and proton tracks in liquid water - II. Nonhomogeneous chemistry, *Radiat. Phys. Chem.* 51 (1998) 245-254. doi: 10.1016/S0969-806X(97)00097-2
- [26] J. Meesungnoen, J.-P. Jay-Gerin, High-LET radiolysis of liquid water with  $^1\text{H}^+$ ,  $^4\text{He}^{2+}$ ,  $^{12}\text{C}^{6+}$ , and  $^{20}\text{Ne}^{9+}$  ions: Effects of multiple ionization, *J. Phys. Chem. A* 109 (2005) 6406-6419. doi: 10.1021/jp058037z
- [27] N. Autsavapromporn, J. Meesungnoen, I. Plante, J.-P. Jay-Gerin, Monte Carlo simulation study of the effects of acidity and LET on the primary free-radical and molecular yields of water radiolysis – Application to the Fricke Dosimeter, *Can. J. Chem.* 85 (2007) 214-229. doi: 10.1139/V07-021
- [28] R. Meesat, S. Sanguanmith, J. Meesungnoen, M. Lepage, A. Khalil, J.P. Jay-Gerin, Utilization of the ferrous sulfate (Fricke) dosimeter for evaluating the radioprotective potential of cystamine: Experiment and Monte Carlo simulation. *Radiat. Res.* 177 (2012) 813-826. doi: 10.1667/RR2829.1
- [29] L. Devroye, *Non-Uniform Variate Generation*, Springer-Verlag, New York, 2000. [luc.devroye.org/rnbookindex.html](http://luc.devroye.org/rnbookindex.html)
- [30] J. von Neumann, *Monte Carlo Method*, National Bureau of Standards Series, vol. 12, pp. 36-38, 1951.
- [31] W.H. Press, S.A. Teukolsky, W.T. Vetterling, B.P. Flannery, *Numerical Recipes in C*, 2<sup>nd</sup> Edition, Cambridge University Press, Cambridge, 1992.
- [32] A.V. Popov, N. Agmon, Three-dimensional simulations of reversible bimolecular reactions: the simple target problem, *J. Chem. Phys.* 115 (2001) 8921-8932. doi: 10.1063/1.1412609
- [33] S. Park, K.J. Shin, A.V. Popov, N. Agmon, Diffusion-influenced excited-state transfer reactions,  $\text{A}^* + \text{B} \leftrightarrow \text{C}^* + \text{D}$ , with two different lifetimes: Theories and simulations, *J. Chem. Phys.* 123 (2005) 034507. doi: 10.1063/1.1948369
- [34] K.M. Hong, J. Noolandi, Solution of the Smoluchowski equation with a Coulomb potential. I. General results, *J. Chem. Phys.* 68 (1978) 5163-5171. doi:10.1063/1.435636
- [35] F.A. Cucinotta, I. Plante, A.L. Ponomarev, M.-H. Kim, Nuclear interactions in heavy ion transport and event-based risk models. *Radiat. Prot. Dosim.* 143 (2011) 384-390. doi: 10.1093/rpd/ncq512

## Appendix I: Green's function

The probability for a pair of particles initially at distance  $r_0$  to be found in the reversible bound state (\*) is given by

$$p^{(*),t|r_0} = \frac{k_a}{k_D r_0} \left[ \frac{\alpha}{(\beta - \alpha)(\gamma - \alpha)} W(\rho_0, -\alpha') + \frac{\beta}{(\gamma - \beta)(\alpha - \beta)} W(\rho_0, -\beta') + \frac{\gamma}{(\alpha - \gamma)(\beta - \gamma)} W(\rho_0, -\gamma') \right]. \quad (\text{A1})$$

The probability for the pair to have reacted and be in the product state (\*\*) is:

$$p^{(**),t|r_0} = \frac{k_a k_e}{r_0 D k_D \alpha \beta \gamma} \left[ \frac{\beta \gamma}{(\beta - \alpha)(\gamma - \alpha)} W(\rho_0, -\alpha') + \frac{\alpha \gamma}{(\gamma - \beta)(\alpha - \beta)} W(\rho_0, -\beta') + \frac{\alpha \beta}{(\alpha - \gamma)(\beta - \gamma)} W(\rho_0, -\gamma') - \text{Erfc}(\rho_0) \right]. \quad (\text{A2})$$

The Green's function for particles in the reversible bound state is also needed. It can be obtained by using the material balance condition  $k_a p(r, t | *) = k_d p(*, t | r)$ . This yields:

$$p(r, t | *) = \frac{k_d}{4\pi r D} \left[ \frac{\alpha}{(\beta - \alpha)(\gamma - \alpha)} W(\rho_r, -\alpha') + \frac{\beta}{(\gamma - \beta)(\alpha - \beta)} W(\rho_r, -\beta') + \frac{\gamma}{(\alpha - \gamma)(\beta - \gamma)} W(\rho_r, -\gamma') \right]. \quad (\text{A3})$$

The dissociation probability (to the reactant state) is given by integrating (A3) over the space where  $r > R$ . This calculation gives:

$$Q(t | *) = \frac{k_d}{RD} \left[ -\frac{1}{\alpha \beta \gamma} + \frac{(R\alpha + 1)}{\alpha(\beta - \alpha)(\gamma - \alpha)} \Omega(-\alpha') + \frac{(R\beta + 1)}{\beta(\gamma - \beta)(\alpha - \beta)} \Omega(-\beta') + \frac{(R\gamma + 1)}{\gamma(\alpha - \gamma)(\beta - \gamma)} \Omega(-\gamma') \right]. \quad (\text{A4})$$

The probability of a pair in a reversibly bound state to remain in this state at time  $t$  is:

$$p^{(*),t|*} = -\frac{\alpha(\beta + \gamma)}{(\beta - \alpha)(\gamma - \alpha)} \Omega(-\alpha') - \frac{\beta(\alpha + \gamma)}{(\gamma - \beta)(\alpha - \beta)} \Omega(-\beta') - \frac{\gamma(\alpha + \beta)}{(\alpha - \gamma)(\beta - \gamma)} \Omega(-\gamma'). \quad (\text{A5})$$

The probability of a pair in a reversibly bound state to react is given by:

$$p^{(**),t|*} = \frac{k_e}{D} \left[ \frac{\alpha + \beta + \gamma}{\alpha \beta \gamma} - \frac{(\beta + \gamma)}{\alpha(\beta - \alpha)(\gamma - \alpha)} \Omega(-\alpha') - \frac{(\alpha + \gamma)}{\beta(\gamma - \beta)(\alpha - \beta)} \Omega(-\beta') - \frac{(\alpha + \beta)}{\gamma(\alpha - \gamma)(\beta - \gamma)} \Omega(-\gamma') \right]. \quad (\text{A6})$$

The reaction rate constants can also be expressed as a function of  $\alpha$ ,  $\beta$  and  $\gamma$ .

$$k_a = -k_D [R(\alpha + \beta + \gamma) + 1], \quad (\text{A7a})$$

$$k_d = \frac{RD(\alpha + \beta)(\beta + \gamma)(\gamma + \alpha)}{R(\alpha + \beta + \gamma) + 1}, \quad (\text{A7b})$$

$$k_e = \frac{D(\alpha\beta + \beta\gamma + \gamma\alpha + R\alpha\beta\gamma)}{R(\alpha + \beta + \gamma) + 1}. \quad (\text{A7c})$$

## Appendix II: Time discretization equations

A simulation is usually divided in a finite number of time steps  $\Delta t$ . If the time  $t$  is the sum of two time steps  $t = \Delta t_1 + \Delta t_2$ , the following possibilities may occur for a pair of particles initially separated by distance  $r_0$ : i) go at distance  $r_1$  during  $\Delta t_1$  and at final distance  $r$  during  $\Delta t_2$ ; ii) go at distance  $r_1$  during  $\Delta t_1$  and bind in a reversible state (\*) during  $\Delta t_2$ ; iii) go at distance  $r_1$  during  $\Delta t_1$  and react to the product state (\*\*) during  $\Delta t_2$ ; iv) reversibly bind during  $\Delta t_1$  and dissociate to the final distance  $r$  during  $\Delta t_2$ ; v) reversibly bind during  $\Delta t_1$  and remain in this state during  $\Delta t_2$ ; vi) reversibly bind during  $\Delta t_1$  and react to the product state during  $\Delta t_2$ ; or vii) react to the product state during  $\Delta t_1$ . This can be expressed mathematically as follows:

$$p(r, \Delta t_1 + \Delta t_2 | r_0) = \int_R^\infty 4\pi r_1^2 p(r, \Delta t_2 | r_1) p(r_1, \Delta t_1 | r_0) dr_1 + p(r, \Delta t_2 | *) p(*, \Delta t_1 | r_0), \quad (\text{B1A})$$

$$p(*, \Delta t_1 + \Delta t_2 | r_0) = \int_R^\infty 4\pi r_1^2 p(*, \Delta t_2 | r_1) p(r_1, \Delta t_1 | r_0) dr_1 + p(*, \Delta t_2 | *) p(*, \Delta t_1 | r_0), \quad (\text{B1B})$$

$$p(**, \Delta t_1 + \Delta t_2 | r_0) = \int_R^\infty 4\pi r_1^2 p(**, \Delta t_2 | r_1) p(r_1, \Delta t_1 | r_0) dr_1 + p(**, \Delta t_2 | *) p(*, \Delta t_1 | r_0) + p(**, \Delta t_1 | r_0). \quad (\text{B1C})$$

Similarly, a pair initially in a reversibly bound state (\*) can i) dissociate to the distance  $r_1$  during  $\Delta t_1$  and go to the final distance  $r$  during  $\Delta t_2$ ; ii) dissociate to the distance  $r_1$  during  $\Delta t_1$  and re-bind reversibly during  $\Delta t_2$ ; iii) dissociate to the distance  $r_1$  during  $\Delta t_1$  and react to the product state during  $\Delta t_2$ ; v) stay reversibly bound during  $\Delta t_1$  and go to the final distance  $r$  during  $\Delta t_2$ ; v) stay reversibly bound during  $\Delta t_1$  and  $\Delta t_2$ ; vi) stay reversibly bound during  $\Delta t_1$  and react to the product state during  $\Delta t_2$ ; or vii) react to the product state during  $\Delta t_1$ . From this the time discretization equations for the pair initially in the reversibly bound state are obtained:

$$p(r, \Delta t_1 + \Delta t_2 | *) = \int_R^\infty 4\pi r_1^2 p(r, \Delta t_2 | r_1) p(r_1, \Delta t_1 | *) dr_1 + p(r, \Delta t_2 | *) p(*, \Delta t_1 | *), \quad (\text{B2a})$$

$$p(*, \Delta t_1 + \Delta t_2 | *) = \int_R^\infty 4\pi r_1^2 p(*, \Delta t_2 | r_1) p(r_1, \Delta t_1 | *) dr_1 + p(*, \Delta t_2 | *) p(*, \Delta t_1 | *), \quad (\text{B2b})$$

$$p(**, \Delta t_1 + \Delta t_2 | *) = \int_R^\infty 4\pi r_1^2 p(**, \Delta t_2 | r_1) p(r_1, \Delta t_1 | *) dr_1 + p(**, \Delta t_2 | *) p(*, \Delta t_1 | *) + p(**, \Delta t_1 | *). \quad (\text{B2c})$$

It was not possible to prove these equations directly by using the analytic expressions of the Green's functions, but they were verified numerically for different values of  $r$ ,  $r_0$ ,  $D$ ,  $\Delta t_1$ ,  $\Delta t_2$ ,  $\alpha$ ,  $\beta$ , and  $\gamma$  (see supporting Mathematica document). In fact, since the Green's functions describe Markov processes, it immediately follows that Chapman-Kolmogorov type equations do hold [19]. As it was discussed in previous work [11,14], these equations offer a way to validate the algorithms presented in this paper, since the simulations are usually done in several time steps.

## Tables

**Table 1.** Average calculation times for 1,000,000 simulation histories (R=1, D=1)

	Reflection ( $k_a=k_d=k_e=0$ )	Diffusion- influenced reactions ( $k_a=4\pi$ , $k_d=k_e=0$ )	Reversible reactions ( $k_a=40\pi$ , $k_d=36$ , $k_e=0$ )	General case ( $k_a=56\pi$ , $k_d=65$ , $k_e=1$ )	General case ( $k_a=12\pi$ , $k_d=4$ , $k_e=5$ )*
Our algorithm	30.1	24.0	45.6	41.1	199.2
<u>Table look-up</u>					
500 bins	24.6	19.6	34.7	32.4	55.9
1,000 bins	34.7	31.1	57.1	51.2	82.0
2,000 bins	69.4	66.0	130.1	126.4	182.7
4,000 bins	218.7	202.2	419.7	424.5	577.3

\*The roots  $\beta$  and  $\gamma$  are complex

**Table 2.** Maximum  $\chi^2$  values for the simulations (R=1, D=1)

	Reflection ( $k_a=k_d=k_e=0$ )	Diffusion- influenced reactions ( $k_a=4\pi$ , $k_d=k_e=0$ )	Reversible reactions ( $k_a=40\pi$ , $k_d=36$ , $k_e=0$ )	General case ( $k_a=56\pi$ , $k_d=65$ , $k_e=1$ )	General case ( $k_a=12\pi$ , $k_d=4$ , $k_e=5$ )*
Our algorithm	106.2	78.5	97.6	100.9	97.2
<u>Table look-up</u>					
500 bins	113.5	122.7	339.7	145.1	157.0
1,000 bins	107.9	96.4	145.2	90.0	112.0
2,000 bins	108.0	103.5	87.7	100.1	89.8
4,000 bins	107.9	96.0	104.3	98.7	118.9

\*The roots  $\beta$  and  $\gamma$  are complex

**Table 3.** Memory usage

	Our algorithm	Table look-up (500 bins)	Table look-up (1,000 bins)	Table look-up (2,000 bins)	Table look-up (4,000 bins)
Memory usage	<0.15 kB	~30 kB	~60 kB	~120 kB	~240 kB

## Figure captions

**Figure 1:** Reflective Green function  $4\pi r^2 p_{ref}(r,t|r_0)$  (Eq. 16) for  $D=1$ ,  $R=1$ ,  $r_0=1.5$  and  $\alpha=-1$ , at  $t=1, 2, 4, 8, 16$  and  $32$ . Analytical functions: (—); Result of sampling: (■).

**Figure 2:** a) Green function of the diffusion-influenced reaction  $4\pi r^2 p(r,t|r_0)$  (Eq. 12) for  $D=1$ ,  $R=1$ ,  $r_0=1.5$  and  $\alpha=-2$  at  $t=1, 2, 4, 8, 16$  and  $32$ . Analytical functions: (—); Result of sampling: (■). b) Average free particle count  $2Q(t|r_0)$  as function of time for  $D=1$ ,  $R=1$ ,  $r_0=1.5$  and  $k_a=4\pi RD$  (—),  $2(4\pi RD)$  (---),  $4(4\pi RD)$  (···) and  $100(4\pi RD)$  (···). Results from IRT simulation: (■).

**Figure 3:** a) Green function for reversible reaction  $4\pi r^2 p(r,t|r_0)$  (Eq. 8) for  $D=1$ ,  $R=1$ ,  $r_0=1.5$ ,  $k_a=10(4\pi RD)$ ,  $k_d=36$  and  $k_e=0$  ( $\alpha=-2$ ,  $\beta=-6$ ,  $\gamma=-3$ ) at  $t=1, 2, 4, 8, 16$  and  $32$ . Analytical functions: (—); Result of sampling: (■). b) Average count of free and reversibly bound particles (given by  $2Q(t|r_0)$  and  $p(*,t|r_0)$ ) as function of time for  $R=1$ ,  $r_0=1.5$ ,  $k_a=5(4\pi RD)$ ,  $k_d=0.5$  (—),  $k_d=5$  (---) and  $k_d=50$  (···). Results from IRT simulation: (■).

**Figure 4:** a) Green function for reversible reaction with intermediate state  $4\pi r^2 p(r,t|r_0)$  (Eq. 8) for  $R=1$ ,  $r_0=1.5$ , for  $k_a=14(4\pi RD)$ ,  $k_d=65$  and  $k_e=1$  ( $\alpha=-8$ ,  $\beta=-2$  and  $\gamma=-5$ ) at  $t=1, 2, 4, 8, 16$  and  $32$ . Analytical functions: (—); Result of sampling: (■). b) Average count of free, reversibly bound and irreversibly bound particles (given by  $2Q(t|r_0)$ ,  $p(*,t|r_0)$  and  $p(**,t|r_0)$ ) as function of time for  $D=1$ ,  $R=1$ ,  $r_0=1.5$ ,  $k_a=4\pi RD$ ,  $k_d=1$  and  $k_e=0.1$  (—),  $k_e=1$  (---) and  $k_e=10$  (···). Results from IRT simulation: (■).

Figure 1

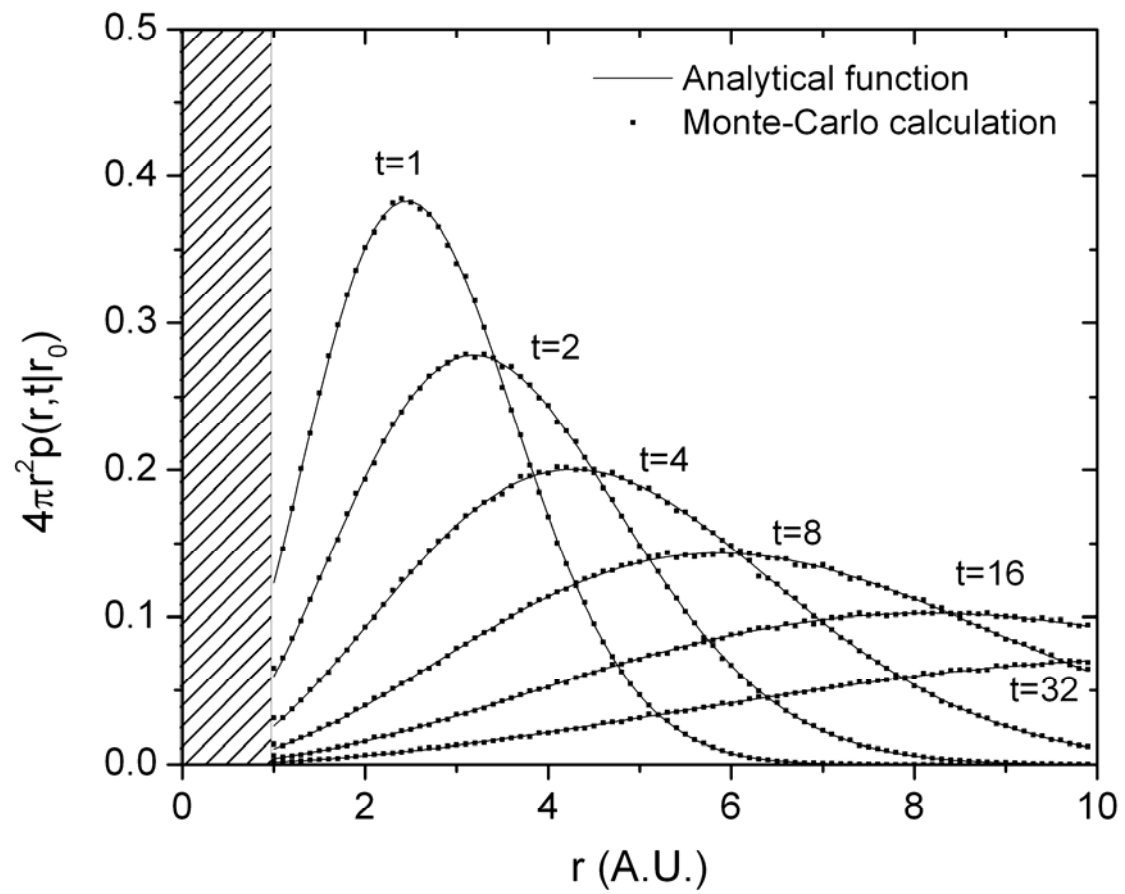


Figure 2

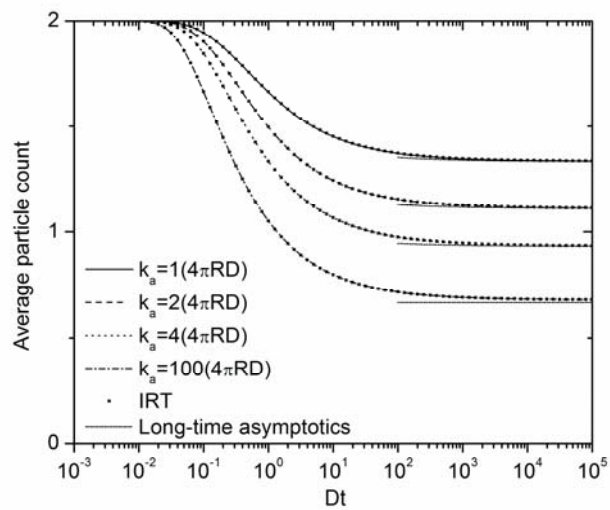
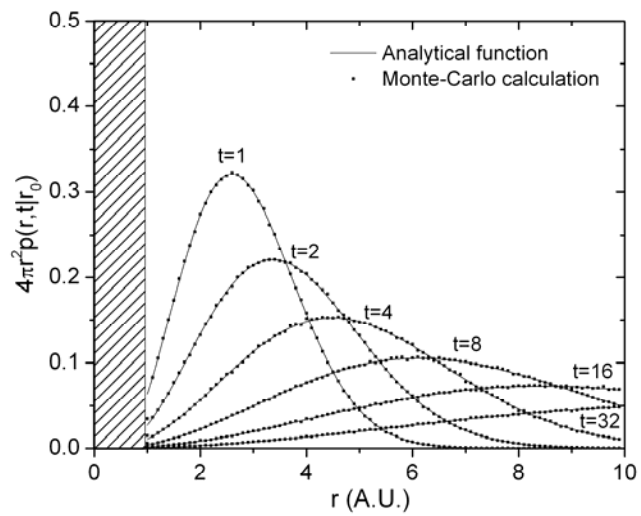


Figure 3

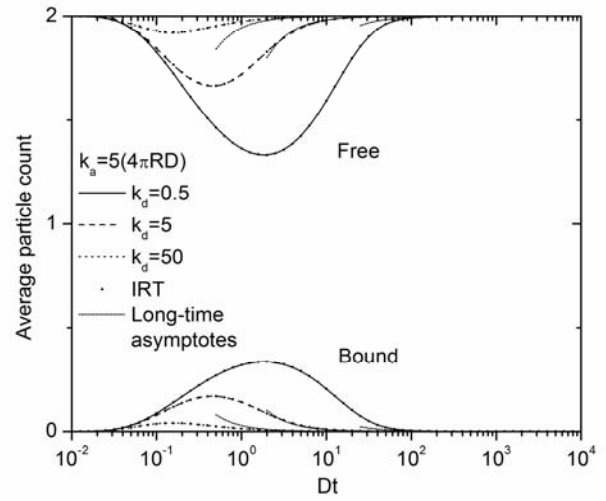
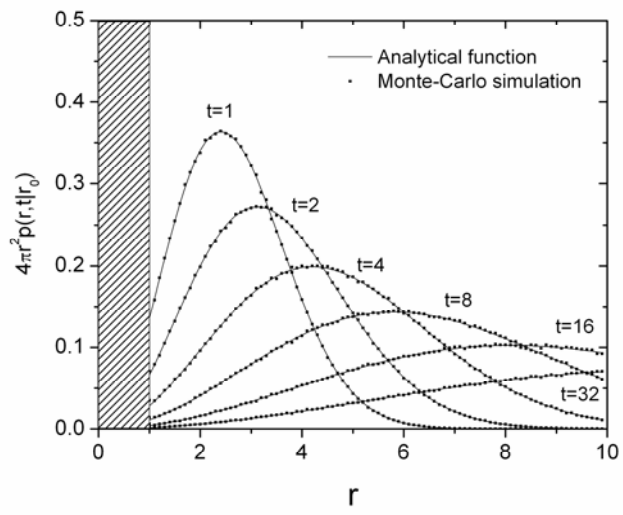


Figure 4

